ROMA: A Database of Rock Reflectance Spectra for Martian In Situ Exploration

L. Mandon, P. Beck, C. Quantin-Nataf, E. Dehouck, P. Thollot, D. Loizeau, M. Volat

AGU ADVANCING EARTH AND SPACE SCIENCE

Earth and Space Science

TECHNICAL REPORTS: DATA
10.1029/2021EA001871

ROMA: A Database of Rock Reflectance Spectra for Martian In Situ Exploration

L. Mandon[1,2], P. Beck[3,4], C. Quantin-Nataf[1], E. Dehouck[1], P. Thollot[1], D. Loizeau[5], and M. Volat[1]

[1]Univ Lyon, Univ Lyon 1, ENSL, CNRS, LGL-TPE, Villeurbanne, France, [2]Now at LESIA, Observatoire de Paris, Université PSL, CNRS, Sorbonne Université, Université de Paris, Meudon, France, [3]Université Grenoble-Alpes, CNRS, IPAG, UMR 5274, Grenoble, France, [4]Institut Universitaire de France, Paris, France, [5]Université Paris-Saclay, CNRS, Institut d'Astrophysique Spatiale, Orsay, France

Key Points:

- We present a database of rock reflectance spectra measured between 0.4 and 3–4 µm
- Similarities in measurement spot size, mineralogy, and rock texture will allow comparisons with analyzes performed on the Martian surface
- This database is made available to the community for future spectral comparisons

Correspondence to:

L. Mandon,
lucia.mandon@obspm.fr

Citation:

Mandon, L., Beck, P., Quantin-Nataf, C., Dehouck, E., Thollot, P., Loizeau, D., & Volat, M. (2022). ROMA: A database of rock reflectance spectra for Martian in situ exploration. *Earth and Space Science*, *9*, e2021EA001871. https://doi.org/10.1029/2021EA001871

Received 2 JUN 2021
Accepted 30 NOV 2021

Author Contributions:

Conceptualization: L. Mandon
Data curation: L. Mandon, C. Quantin-Nataf, M. Volat
Formal analysis: L. Mandon, P. Thollot, D. Loizeau
Funding acquisition: P. Beck, C. Quantin-Nataf
Investigation: L. Mandon
Methodology: L. Mandon, P. Beck, C. Quantin-Nataf, E. Dehouck
Supervision: P. Beck, C. Quantin-Nataf, E. Dehouck
Visualization: L. Mandon, M. Volat
Writing – original draft: L. Mandon

Abstract The ROMA database (ROck reflectance for MArtian in situ exploration, https://roma.univ-lyon1.fr) provides the reflectance spectra between 0.4 and 3–4 µm of various terrestrial, Martian, and synthetic samples, as a means to document reference measurements for comparison with data acquired by visible and near-infrared spectrometers on planetary surfaces, with a focus on current and future Martian observations by the Perseverance (Mars 2020 mission) and Rosalind Franklin (ExoMars) rovers. The main specificity of this database is to include a significant fraction of spectra of unprocessed rock, which are more realistic analogs and often have different spectral features than the fine powders more commonly analyzed in reflectance spectroscopy. Additionally, these measurements were acquired with a spectrometer whose spot size is similar to those of the SuperCam instrument (Mars 2020 mission) at a few meters from a target. Supplementary information are provided in the ROMA database: higher-level data (such as absorption band parameters) as well as sample mineralogy estimated by whole-rock X-ray diffraction analyses. Future comparisons with this database will help improve the interpretation of spectral measurements acquired on the Martian surface. This work introduces the aim of the library and its current state, but additional data on intact natural rock surfaces will likely be added in the future.

1. Introduction

Reflectance spectroscopy is a nondestructive technique that is widely used to remotely investigate the mineralogical composition of rocks and, more generally, planetary surfaces. Spectral libraries are the main references used to interpret these spectra and assess the mineralogical composition of the analyzed surface. It is therefore crucial for databases to include: (a) well-documented samples, in particular through additional analyses with techniques complementary of reflectance spectroscopy and (b) samples that share characteristics with the rock samples of unknown composition being measured with reflectance spectroscopy. This includes the elemental and mineralogical composition of the sample, but also its physical properties such as grain size, surface roughness, and porosity, which are known to greatly affect the absolute reflectance values and band depths (e.g., Clark & Roush, 1984). Especially, it has been demonstrated that rocks have different spectral signatures compared to particulate surfaces (e.g., Carli et al., 2015; Harloff & Arnold, 2001; Pompilio et al., 2007). While the spectra of a wide range of minerals of various compositions are well documented in the current databases, most of these measurements were performed on powders, with a majority of them being pure or nearly pure mineral phases (e.g., Kokaly et al., 2017). The complex effects of grain size, roughness, or impurities on natural rocks reflectance have been approached in the literature (e.g., Carli & Sgavetti, 2011; Carli et al., 2015; Clark & Roush, 1984; Harloff & Arnold, 2001), but well-documented rock spectra are nonetheless needed for the planetary science community in order to fully understand the spectral behavior of planetary surfaces.

In early 2021, the Perseverance rover of the Mars 2020 mission (NASA) landed on Mars, carrying on board the first reflectance point spectrometer covering the dedicated visible and near-infrared (VNIR) spectral range: the Infrared Spectrometer (IRS) of the SuperCam instrument (Fouchet et al., 2021; Maurice et al., 2021). In 2023, the ExoMars mission (ESA/Roscosmos) will bring the first VNIR imaging spectrometer on the surface of Mars, MicrOmega (Bibring et al., 2017), as well as two other point spectrometers, Ma_MISS and ISEM (De Sanctis et al., 2017; Korablev et al., 2017). All these instruments are dedicated to the mineralogical characterization of

Writing – review & editing: L. Mandon, P. Beck, C. Quantin-Nataf, E. Dehouck, D. Loizeau

rocks and soils, which are complex mixtures of various mineralogical phases: a comparison with well-documented rock spectra would improve the interpretation of these surface measurements.

The main spectral libraries including measurements of intact rocks are the Reflectance Experiment Laboratory facility (RELAB; Pieters & Hiroi, 2004) and the database of the Centre for Terrestrial and Planetary Exploration (C-TAPE, formerly known as HoserLab; Cloutis et al., 2006). In particular, a fraction of the rocks measured at the C-TAPE facility is associated with mineralogical and elemental compositions, but at the time of writing of this manuscript, photographs showing the corresponding measurement spots were not provided in any of the databases. The Solid Spectroscopy Hosting Architecture of Databases and Expertise (SSHADE; Schmitt et al., 2014) also provides some spectral measurements of intact rocks in the visible and infrared, but they comprise a minor fraction of the database. Finally, the more recent Planetary Terrestrial Analogs Library Project (PTAL) is being built with Martian whole-rock analogs characterized with various techniques already used on the Martian surface and including reflectance spectroscopy (Dypvik et al., 2021). However, all of the samples were ground prior to the reflectance measurements (Lantz et al., 2020).

In this contribution, we present the ROMA (ROck reflectance for MArtian in situ exploration) database, which regroups a set of spectral measurements between 0.4 and 3–4 μm on intact and particulate rocks—most of them have had their mineralogy characterized using X-ray diffraction (XRD) on ground samples. This collection currently includes a set of terrestrial samples with various degrees of alteration, Martian meteorites, as well as synthetic mixtures of minerals detected over the landing sites and compacted into solid pellets. The latter are not perfect analogs to simulate rock textures, but expand the spectral library of nonparticulate materials that are relevant to planetary exploration. The reflectance spectra of these samples are provided, along with higher-level data, such as continuum-removed spectra and absorption band parameters, which are mostly influenced by rock composition, grain size, porosity, and roughness. Comparisons with this database will aid the interpretation of reflectance measurements performed on the Martian surface.

2. The ROMA Database

The sample and spectral information in ROMA are regrouped into an SQLite database in which three tables are connected: a table that contains the sample information and two tables of reflectance and XRD data that either include VNIR spectra or diffractograms of these samples, measurement conditions, and higher-level data (Figure 1). In the following sections, each table is presented in details, along with the list of samples included in the database and the methodology employed to obtain the VNIR spectra and diffractograms of the samples.

2.1. Samples

As of the beginning of 2021, the ROMA database documents the VNIR spectra of 27 Martian meteorites and 132 Mars analog samples: 64 terrestrial rocks and 68 unique synthetic pellets. When grinding was possible, reflectance spectra were acquired on powdered samples in addition to the ones acquired on unprocessed rocks. To ensure agreement between the powder (both used for XRD and reflectance observation) and the intact rock measurements, homogeneous areas of the rocks were considered, both for the reflectance acquisition on the chip and for sampling of the area to be crushed for powder preparation. A measurement area was considered representative of the rock when including all the apparent features used for a first-level description (e.g., the presence of a groundmass, phenocrysts, vein, etc.). When a sample displayed a heterogeneous texture, several measurements were performed on the rock. For example, the basalt SL4-5 exhibits a coating; in this case, a measurement was performed on the broken interior of the rock as well as on the patina.

2.1.1. Martian Meteorites

The reflectance spectra of 27 Martian meteorites are included in the database: 18 shergottites, five nakhlites, one chassignite, as well as the unique specimens of the augite-rich basalt NWA 8159, the polymict breccia NWA 7034 and the orthopyroxenite ALH 84001. Most of these precious and rare samples are chips of rocks and were not ground to perform whole-rock XRD measurements; however, their mineralogical and chemical compositions are well documented in the literature (e.g., Beck et al., 2006; Herd et al., 2017; Sautter et al., 2002). A study dedicated to the investigation and interpretation of the spectral features of their reflectance spectra was performed by Mandon et al. (2021a).

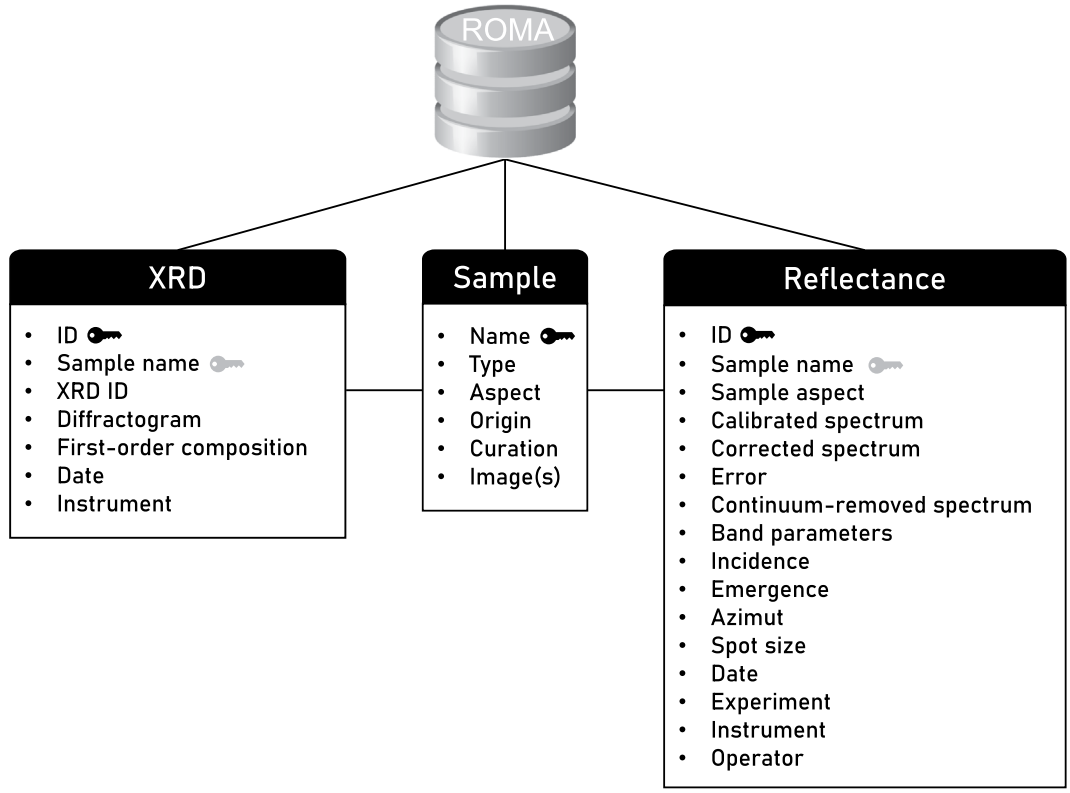

Figure 1. Current architecture of ROMA. The database is divided into three main tables: the "Sample," "Reflectance," and "X-ray diffraction (XRD)" tables. Each table includes a variety of fields that can either contain an integer, some text, or a binary object (e.g., an image). The black key indicates an entry that is unique in the table, while the gray keys point to fields inherited from the "Name" field of the "Sample" table, meaning that each unique sample can be associated with multiple reflectance and XRD measurements. An access to these information is provided at https://roma.univ-lyon1.fr.

2.1.2. Terrestrial Rocks

The terrestrial rocks present in the database were collected in the geological collections of the Observatoire de Lyon or during field campaigns and come from various locations in France.

Many geological units potentially of magmatic origin are identified at the Mars 2020 and ExoMars landing sites (e.g., Goudge et al., 2015; Quantin-Nataf et al., 2021). Most of these units exhibit the spectral signatures of mafic minerals, such as pyroxene and olivine (Goudge et al., 2015; Hoefen et al., 2003). More globally, spectral measurements on meteorites and from orbit indicate that the Martian crust is dominantly of basaltic composition (e.g., McSween et al., 2009). However, minerals enriched in silica are usually difficult to detect using VNIR spectroscopy (Crown & Pieters, 1987) and evolved lithologies have been observed in situ while not being detected from orbit (Sautter et al., 2015). Consequently, most of the igneous rocks present in the database are basaltic rocks, but in order to account for the potential presence of evolved rocks on the landing sites, a wider range of lithologies (e.g., andesite, trachyte, dacite) has been investigated (Table 1). Both rocks that exhibit aphanitic and phaneritic textures are present in the suite, meaning that rocks with various grain sizes are included in the library.

In addition to these igneous rocks, the library includes sedimentary samples, mineralized veins, or rocks in which the primary texture has been lost or strongly modified by alteration. The majority of these samples are paleosols (i.e., rocks altered by pedogenesis processes). They were sampled during two field campaigns:

1. rocks with name starting with "SL" were sampled on various levels of altered basaltic flows in Loire and Velay, France. For exact location of sampling and outcrop photographs, the reader is referred to Mandon (2020) and to the database website, which can be accessed at http://roma/univ-lyon1.fr
2. rocks with name starting with "R" or "S" were sampled in the "Ocres de Roussillon," France, on sedimentary rocks altered by pedogenesis (Guennelon, 1962)

Table 1
List of the Samples Present in the ROMA Database as in Early 2021

ROMA ID	Type	ROMA ID	Type	ROMA ID	Type	ROMA ID	Type
Terrestrial rocks		SL1-0b	Clay inclusion	NWA12633	Shergottite	ol_carb_ serp_020_040_040	Mixture
UCB15	Andesite	SL1-4	Detritical sand	NWA12960	Shergottite	ol_carb_ serp_020_060_020	Mixture
UCB16	Andesite	SL1-5	Detritical sand	NWA12965	Shergottite	ol_carb_ serp_020_080_000	Mixture
LM16	Basalt	SL4-1	Detritical sand	SaU008	Shergottite	ol_carb_ serp_040_000_060	Mixture
SL1-0	Basalt	SL4-2	Nontronite soil	Tissint	Shergottite	ol_carb_ serp_040_020_040	Mixture
SL4-3	Basalt	SL4-7	Nontronite soil	Zagami	Shergottite	ol_carb_ serp_040_040_020	Mixture
SL4-4	Basalt	R1P2	Paleosol			ol_carb_ serp_040_060_000	Mixture
SL4-5	Basalt	R2P3	Paleosol	*Synthetic pellets*		ol_carb_ serp_060_000_040	Mixture
SL4-6	Basalt	R7P2	Paleosol	mont_kaol_000_100	Mixture	ol_carb_ serp_060_020_020	Mixture
SL4-12	Basalt	SL1-2	Paleosol	mont_kaol_001_099	Mixture	ol_carb_ serp_060_040_000	Mixture
SL4-13	Basalt	SL1-3	Paleosol	mont_kaol_005_095	Mixture	ol_carb_ serp_080_000_020	Mixture
SL4-14	Basalt	SL1-3b	Paleosol	mont_kaol_010_090	Mixture	ol_carb_ serp_080_010_010	Mixture
UCB22	Basalt	SL1-3t	Paleosol	mont_kaol_020_080	Mixture	ol_carb_ serp_080_020_000	Mixture
UCB23	Basalt	SL4-10	Paleosol	mont_kaol_040_060	Mixture	ol_carb_ serp_090_000_010	Mixture
LM17	Basaltic sand	S1P2	Pelite	mont_kaol_060_040	Mixture	ol_carb_ serp_090_005_005	Mixture
UCB10	Dacite	S1P3	Pelite	mont_kaol_080_020	Mixture	ol_carb_ serp_090_010_000	Mixture
UCB11	Dacite	SL3-1	Pelite	mont_kaol_090_010	Mixture	ol_carb_ serp_095_000_005	Mixture
PL_C3	Diorite	SL3-2	Pelite	mont_kaol_095_005	Mixture	ol_carb_ serp_095_005_000	Mixture
UCB7	Diorite	SL1-1	Peperite	mont_kaol_099_001	Mixture	ol_carb_ serp_099_000_001	Mixture
PL_E8	Gabbro	UCB1	Serpentinite	mont_kaol_100_000	Mixture	ol_carb_ serp_099_001_000	Mixture
PL_B1	Gabbro	UCB4	Serpentinite	ol_carb_ serp_000_000_100	Mixture	ol_carb_ serp_100_000_000	Mixture
PL_B2	Gabbro			ol_carb_ serp_000_001_099	Mixture	ol_verm_000_100	Mixture
UCB8	Gabbro	*Martian meteorites*		ol_carb_ serp_000_005_095	Mixture	ol_verm_001_099	Mixture
UCB9	Gabbro	NWA8159	Augite basalt	ol_carb_ serp_000_010_090	Mixture	ol_verm_005_095	Mixture
PL_D5	Granodiorite	NWA2737	Chassignite	ol_carb_ serp_000_020_080	Mixture	ol_verm_010_090	Mixture

Table 1
Continued

ROMA ID	Type	ROMA ID	Type	ROMA ID	Type	ROMA ID	Type
PL_B5	Monzogranite	CeC022	Nakhlite	ol_carb_serp_000_040_060	Mixture	ol_verm_020_080	Mixture
PL_D12	Monzogranite	Lafayette	Nakhlite	ol_carb_serp_000_060_040	Mixture	ol_verm_040_060	Mixture
UCB2	Peridotite	MIL03346	Nakhlite	ol_carb_serp_000_080_020	Mixture	ol_verm_060_040	Mixture
UCB3	Peridotite	Nakhla	Nakhlite	ol_carb_serp_000_090_010	Mixture	ol_verm_080_020	Mixture
IPAG1	Peridotite	NWA817	Nakhlite	ol_carb_serp_000_095_005	Mixture	ol_verm_090_010	Mixture
UCB19	Phonolite	ALH84001	Orthopyroxenite	ol_carb_serp_000_099_001	Mixture	ol_verm_095_005	Mixture
UCB20	Phonolite	NWA7034	Polymict breccia	ol_carb_serp_000_100_000	Mixture	ol_verm_099_001	Mixture
UCB17	Rhyolite	ALH77005	Shergottite	ol_carb_serp_001_000_099	Mixture	ol_verm_100_000	Mixture
UCB18	Rhyolite	DaG476	Shergottite	ol_carb_serp_001_099_000	Mixture		
PL_A3	Syenogranite	DaG489	Shergottite	ol_carb_serp_005_000_095	Mixture	*Minerals used in mixtures*	
PL_G37	Syenogranite	EETA79001	Shergottite	ol_carb_serp_005_005_090	Mixture	LM1	Olivine (forsterite)
UCB14	Trachyandesite	Los Angeles	Shergottite	ol_carb_serp_005_090_005	Mixture	LM3	Carbonate (magnesite)
UCB12	Trachyte	NWA480	Shergottite	ol_carb_serp_005_095_000	Mixture	LM15	Serpentine (antigorite)
UCB13	Trachyte	NWA1068	Shergottite	ol_carb_serp_010_000_090	Mixture	KGa-2	Kaolinite
SL4-9	Burned clays	NWA1195	Shergottite	ol_carb_serp_010_010_080	Mixture	SWy-3	Montmorillonite
SL4-8	Burned soil	NWA1950	Shergottite	ol_carb_serp_010_080_010	Mixture	UCB24	Vermiculite
SL1-0t	Calcite vein	NWA4468	Shergottite	ol_carb_serp_010_090_000	Mixture		
SL4-5p	Varnish on basalt	NWA4766	Shergottite	ol_carb_serp_020_000_080	Mixture		
SL4-11	Clay and oxide-rich vein	NWA7397	Shergottite	ol_carb_serp_020_020_060	Mixture		

2.1.3. Synthetic Pellets

In addition to terrestrial and Martian rocks, our database also includes the reflectance spectra of synthetic samples of simplified composition and mineralogy that are directly comparable to those estimated on the Mars 2020 and ExoMars landing sites from orbit. As ROMA is a database focused on the reflectance of rocks (as opposed to powders), mixtures of pure minerals were compressed into solid pellets (Figure 3b). These samples are not perfect analogs to mimic rock textures, but are here used to evaluate the spectral properties of mixtures in a medium with reduced porosity and compacted grains.

The mixed samples were selected based on their relevance for the Martian sites explored (see Section 3) and their mineralogical purity, estimated with XRD (see Section 2.3). Three types of mixtures analog to the landing sites were produced (Table 1):

1. olivine (forsterite) mixed with Fe/Mg-clay mineral (vermiculite), assemblage likely present in the region of the ExoMars landing site (Mandon et al., 2021c)
2. olivine (forsterite) mixed with Mg-carbonate (magnesite) and serpentine (antigorite), assemblage likely present in the region of the Mars 2020 landing site (Ehlmann et al., 2008, 2009; Hoefen et al., 2003)
3. montmorillonite mixed with kaolinite, assemblage likely present in the region of the Mars 2020 and ExoMars landing sites (Carter et al., 2016; Ehlmann et al., 2009). These two samples are well characterized natural standards from the Clay Minerals Society (e.g., Chipera & Bish, 2001; Moll, 2001)

Diffractograms acquired on powders of the samples used in the mixtures are available in the database (see Section 2.3).

Reflectance measurements on mineral mixtures have already been performed for similar species (e.g., Bishop et al., 2013; McKeown et al., 2011), but not on compacted samples. In addition, mixtures of highly uneven ratios (e.g., 1:99 or 5:95) were rarely studied, even though certain absorption bands are known to appear at low mineralogical proportion (e.g., Thollot, 2013). Here, the mixtures were produced in fractions which allow the investigation of the effect of minor mineralogical proportions on reflectance spectra: 0:100, 1:99, 5:95, 10:90, 20:80, 40:60, 60:40, 80:20, 90:10, 95:5, 99:1, and 100:0. The resulting data sets include 12 pellets in the case of binary mixtures and 45 in the case of ternary mixtures (using the same proportion values).

In order to produce the pellets, selected minerals were first ground in a mechanical agate miller and sieved to retain grains with size inferior to 100 µm. A significant fraction of coarse (∼1 mm) grains was inferred from orbit for the olivine widely present at the Mars 2020 landing site (Poulet et al., 2009), and some spectra measured over the ExoMars landing site are consistent with fayalite or coarse-grained forsterite (Mandon et al., 2021c). Therefore, a coarser grain size was chosen for the olivine in the mixtures (0.1–1 mm). The resulting pure mineral powders were mixed by weight according to the mixing ratios described above. About 500 g of each homogenized powder mixture was inserted into a pellet press and heated at 30°C to remove excess water from the sample. After 20 min, 10 tons pressure was applied during 30 min, in order to produce the pellets analyzed with the reflectance spectrometer. This pressure allows compaction of pellets without mineralogical transformation.

2.2. VNIR Reflectance Spectra

The ROMA database includes the calibrated reflectance spectra of the samples ("calibrated spectrum" field) along with measurement information and associated errors (Figure 1; see Potin et al., 2018 on errors). Higher-level data are also provided: smoothed spectra corrected from recurring artifacts ("corrected spectrum" field), continuum-removed spectra and quantitative parameters of the main absorption bands (Figure 1).

2.2.1. Spectral Acquisition

The VNIR reflectance of every sample in the ROMA database was measured between 0.4 and 3–4 µm at a spectral sampling of 10 or 20 nm and with a varying spectral resolution (on the order of 10 nm) by the Spectrophotometer with cHanging Angles for the Detection Of Weak Signals (SHADOWS; Potin et al., 2018). This setup provides the possibility of varying the geometry of illumination and observation, whose parameters are the incidence, emergence, and azimuth angles, following the convention described by Potin et al. (2018). The incidence angle is the angle between the normal to the surface and the incident beam and the emergence angle is the angle between the normal to the surface and the direction of observation. The azimuth is the angle between the plane defined by the normal to the surface and the incident beam, and the plane defined by the normal to the surface and the direction of observation. The incident light is generated by a quartz tungsten-halogen lamp and filtered at a different wavelength for each time step using a four-gratings monochromator. The light focused on the output slit is cleaned from chromatic aberrations using torus mirrors and high-pass filters are used to remove high-order reflections and stray light. This monochromatic beam is transported through eight optical fibers and focused on the sample, while the light emerging from the sample is measured by two detectors, covering the 0.185–1.2 and 0.8–5.2 µm spectral ranges respectively (Potin et al., 2018). As most of the absorptions related to minerals are comprised in the 0.4-µm to 3–4-µm range, the spectral measurements included in ROMA were not performed over the full range covered by the detectors.

As the illumination and observation half-angles are, respectively, 2.9 and 2°, the setup geometry is bidirectional rather than biconical. Except for the NWA 4766 meteorite, all the spectral measurements were performed

with an emergence angle of 30° and under nadir illumination, resulting in a ∼5.2-mm wide illumination spot (Figure 3a). This value is similar to the field of view of SuperCam's IRS when the instrument is at ∼2–4 m from a target (Wiens et al., 2021). The NWA 1195 and NWA 8159 meteorites were too small to be illuminated by all eight optical fibers and a pinhole was placed to filter the incident light and reduce the spot size down to ∼1.3 mm × ∼1.7 mm. For rock samples, the location and approximate size of the illumination spot are reported in the sample sheet of the library website. As in this setup a fiber bundle is used to illuminate the samples, it should be noted that the measurement spot is not uniformly illuminated. In addition, the field of view of the instrument is larger than the illumination spot, and the lock-in amplifiers used might not entirely remove the entire thermal emission and light scattered by the sample and the sample holder.

Spectra of highly reflective reference targets were acquired for each day of measurement and used to calibrate the data in real-time during the acquisition: a Spectralon™ target below ∼2.2 µm and an Infragold™ target for the rest of the spectral range. A correction accounting for the non-Lambertian behavior of these reference targets was included in the calibration process (Potin et al., 2018).

2.2.2. SNR and Main Artifacts

The SHADOWS point spectro-goniometer is able to measure the reflectance of a sample in the VNIR down to 0.005% in reflectance, with 1% accuracy and with varying illumination and emergence angles (Potin et al., 2018). This high sensitivity allows excellent signal-to-noise ratio (SNR), usually exceeding 100–1,000 in the VNIR range for most of the rocks measured, which hence permits the detection of absorption bands at a 0.1–1% precision relative to the spectral continuum. While, the SNR values are usually higher than 100–1,000 over the whole spectral range, they can be lower in the case of dark samples. The near-infrared detector produces data with SNR one to three orders lower than in the case of the visible detector and an SNR drop corresponding to the detector switch is observed at 1 µm.

While most of the following artifacts are removed from the data (see Section 2.2.3), users of the library should be careful about possible remaining artifacts that were not identified during the correction:

1. misalignment between detectors, wrong level of a sample or issue with the gratings' rotation can lead to reflectance shifts at wavelengths corresponding to detector or grating switch: at 0.68, 1, 1.4, and 3.6 µm
2. isolated spikes in reflectance (restricted to one spectel) can be observed. The origin of these artifacts is not yet fully understood but might be related to a cryocooler issue.
3. changes of water vapor pressure in the room between the spectral acquisition of the calibration targets and the sample as well as water adsorbed on the sample surface might lead to additional absorption bands related to the vibration of water molecules (at ∼1.4, ∼1.9, and ∼3 µm)

2.2.3. Higher-Level Data

In addition to the calibrated spectra, smoothed and corrected from artifacts spectra are usually provided, along with continuum-removed spectra (CRS) and observed band parameters values. The processing performed to generate corrected spectra is as follows.

1. Identified artifacts are corrected from the calibrated data: parts of the spectra where shifts in reflectance values at detectors and gratings changes are observed (see Section 2.2.2) are correctly realigned in reflectance. In case of reflectance offset between the visible and infrared detector, the infrared range was realigned based on the reflectance measured by the visible detector, which has a higher flux. Spikes restricted to isolated spectels and narrow water vapor bands are extrapolated by averaging from neighbors spectels
2. if needed, smoothing of the spectra is performed using a Savitzky-Golay filter with a moving window adapted to each spectrum and depending on the SNR
3. finally, the spectra are oversampled at 1 nm using a cubic interpolation, as a means to refine the band parameter values retrieval. The resulting data are labeled as “corrected”

The corrected spectra are divided by a fitted continuum to produce the CRS. The corresponding method is described in details by Mandon, Beck, Quantin-Nataf, Dehouck, Pommerol, et al. (2021) and varies depending on the spectral shape of each corrected spectrum. When only broad absorptions (usually related to the presence of mafic minerals) are observed, the continuum is estimated using the method described by Horgan et al. (2014), where a set of continuums between defined ties is generated. For each band, the continuum that maximizes the

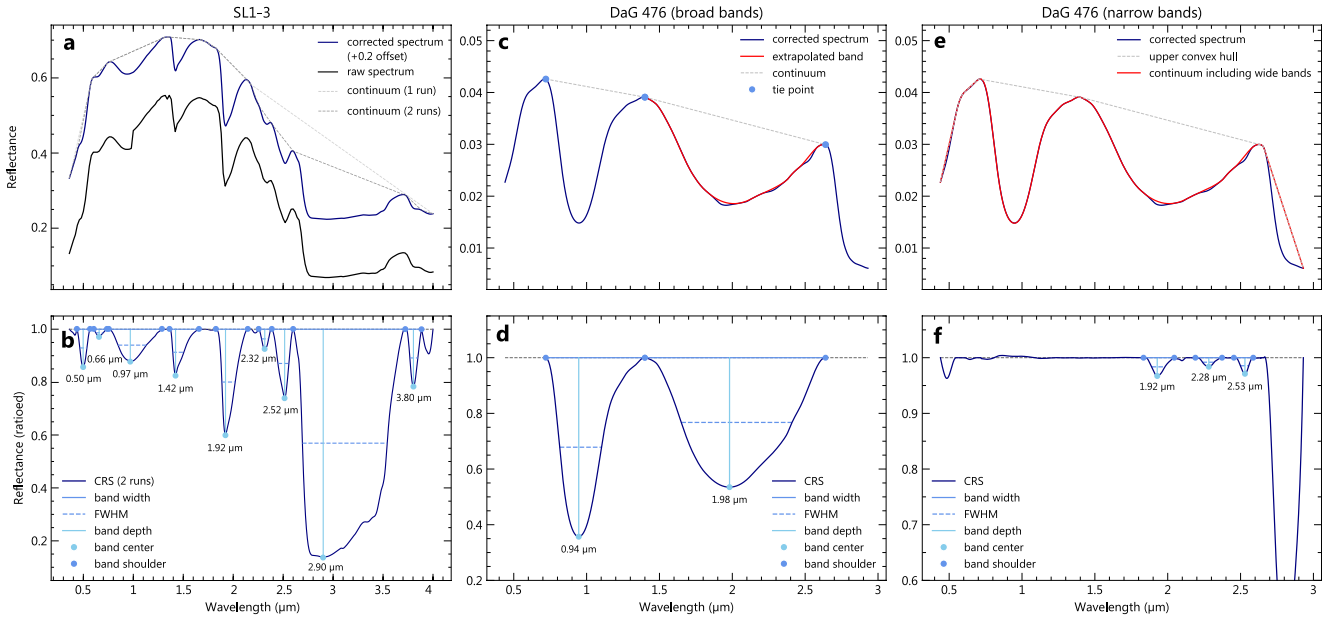

Figure 2. Example of continuum fitting and absorption band parameters retrieval (from Mandon, Beck, Quantin-Nataf, Dehouck, Pommerol, et al., 2021, modified). (a, b) For the reflectance spectrum of SL1-3, two steps of upper convex hull wrapping are used to fit a continuum allowing the extraction of all the observed absorption bands. (c, d, e, f) For the spectrum of DaG476, narrow bands at 1.92, 2.28, and 2.53 µm superimpose a broad absorption centered at 1.98 µm. Hence, a first continuum defined by tie points maximizing the areas of the broad ∼1 and 2 µm absorptions is estimated and used to extract their band parameters, excluding the narrow absorptions. Then, the estimated reflectance of the 1.98-µm band is used as a continuum to extract the parameters of the narrow bands.

absorption area is kept for continuum removal. For spectra showing narrow absorption bands only (usually when secondary minerals are present), the continuum is simply estimated using the upper part of the convex hull of the spectrum. This method rarely allows all absorption bands to be wrapped and was repeated until a satisfactory result was obtained (Figures 2a and 2b). Whenever narrow absorption bands overlap the broad bands of mafic minerals, a first continuum is removed to extract the broad band parameters according to the first method described (Figures 2c and 2d), where narrow absorption bands are excluded. The broad bands detected are then included to the convex hull of the initial spectrum, so as to form a continuum which allows the narrow absorption bands extraction only (Figures 2e and 2f; Mandon, Beck, Quantin-Nataf, Dehouck, Pommerol, et al., 2021).

Each line of the ROMA "band parameters" field contains the band parameters extracted from the CRS, in the following arrangement: position, depth, width, area, and Full Width at Half Maximum (FWHM).

2.3. XRD Characterization of the Samples

In order to estimate the mineralogical assemblages of the samples, whole-rock X-ray diffraction (XRD) analyses were performed at the Centre de Diffractométrie Henri Longchambon. The XRD technique requires grinding of a few tens of grams for each sample. Diffractograms were acquired in the 3–70° 2θ range using a Bruker D8 Advance Bragg-Brentano diffractometer (40 kV/40 mA Cu tube) with variable divergence slits and using the Cu K_{α} radiation, at 0.0205° 2θ step and 0.4-s time step.

The diffractograms analysis was carried out using the DIFFRAC.EVA software suite. A peak comparison with the PDF-4 database allowed phase identification and semiquantification with the Reference Intensity Ratio (RIR) method (Hubbard & Snyder, 1988). Semiquantification on whole-rock analysis is time-efficient and allows the investigation of a large collection of samples, but can lead to large uncertainties in the quantification results, especially if phyllosilicate peaks are present. Considering these limitations, the mineralogical assemblage estimation is available in ROMA as a "first-order composition," as follows: <15%: "+," 15–30%: "++," 30–60%: "+++," and >60%: "++++."

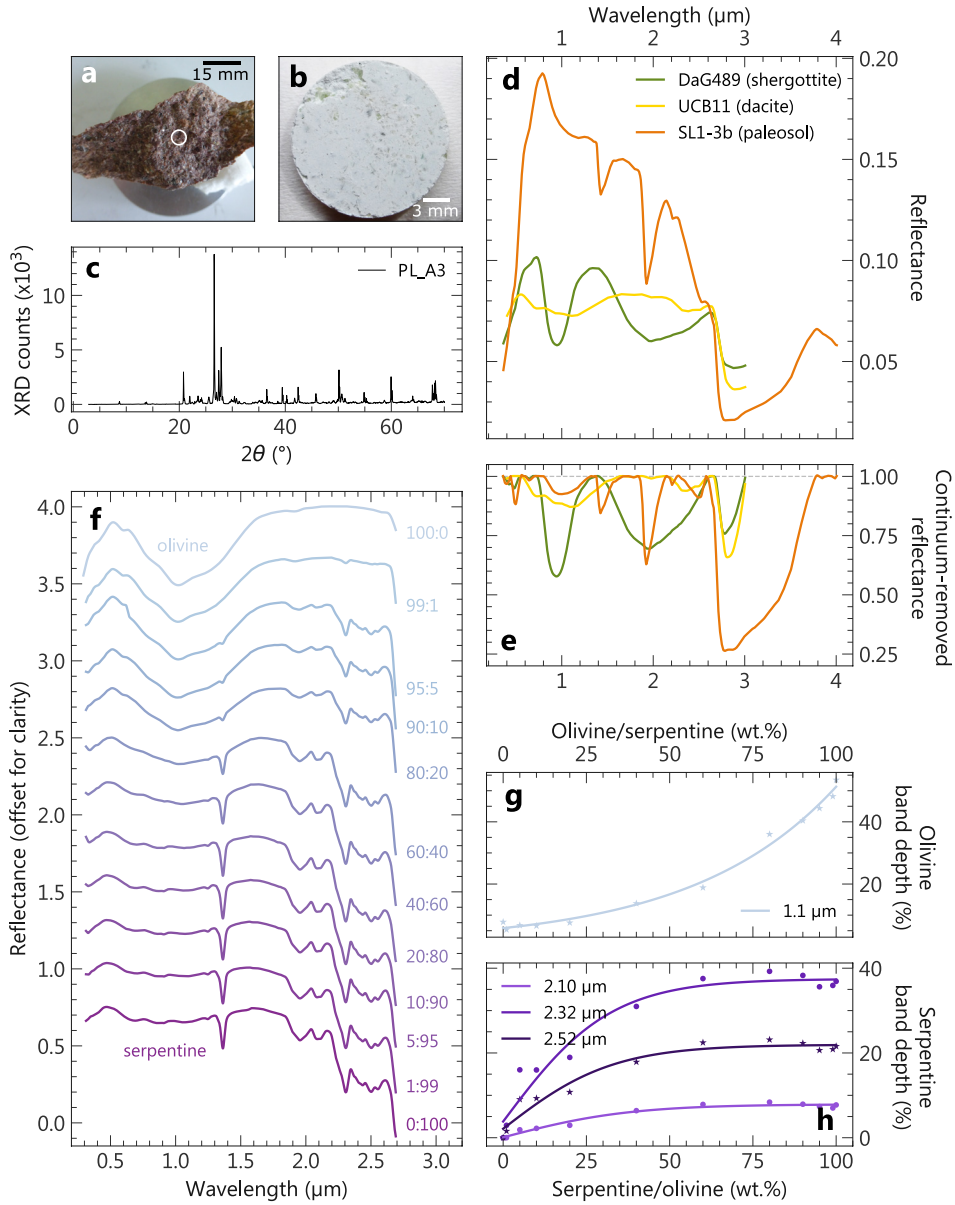

Figure 3. Examples of samples and products included in the ROMA database. (a) Sample UCB18 (rhyolite), with corresponding VNIR spectral spot measurement. (b) Compressed pellet of a mixture of 60 wt.% serpentine and 40 wt.% olivine. (c) XRD diffractogram measured on sample PL_A3 (syenogranite). (d) Corrected reflectance spectra and (e) continuum-removed spectra of three samples from the database. (f) Reflectance spectra of pellet mixtures of olivine and serpentine (proportions in wt.%). (g) Evolution of the depth of the absorption band related to olivine in the olivine/serpentine mixture samples. (h) Evolution of the depth of three absorption bands related to serpentine in the olivine/serpentine mixture samples.

3. Potential Applications to Martian Measurements

ROMA aims at providing an additional framework for future comparisons with in situ measurements performed on the Martian surface by VNIR spectrometers. The specificity of the database is to provide spectra measured on whole-rocks, both intact and ground to powder, as well as synthetic mixtures of Martian analogs, and to include XRD measurements as well as absorption band parameters (e.g., position, depth), which are information that are meaningful in terms of mineralogical assemblage. A comparison with the band parameters values might be helpful for estimating the composition of a Martian target of unknown nature.

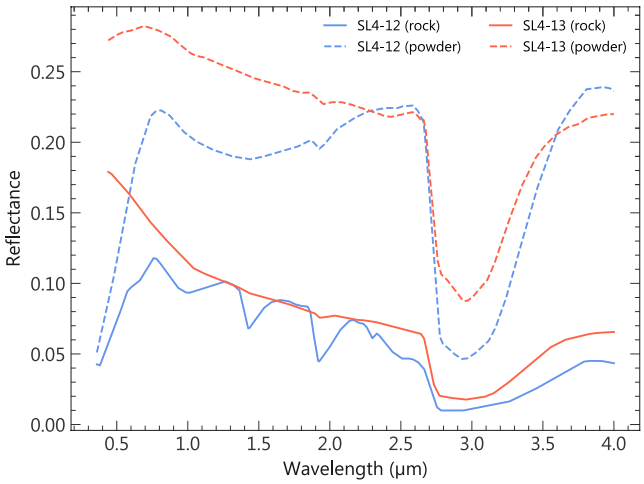

Figure 4. Example of spectra measured on a particulate and rock version of the same samples.

Figure 4 illustrates how particulate and intact rock samples of the same material can behave very differently. For both types of samples shown here, variations of absorption strength and spectral slopes are observed (with the rock samples being bluer in the VNIR), but more interestingly, it should be noted that the absorption bands observed in one type of sample are not necessarily observed in the other one. Here, SL4-12 is a basalt with vesicles filled with secondary phases, mostly nontronite in the field of view of the measurement. While the absorptions related to nontronite (at ~1, 1.42, 1.92, and 2.28 μm) are present in the rock spectrum, they are not anymore observed after grinding as the signature of the groundmass dominates. It is not excluded that similar differences might be observed between the spectrum of a drilled rock and the spectrum of its corresponding drill tailings, while having the same mineralogical composition. Having access to the type of measurements included in ROMA would hence provide additional context to understand in situ spectral signatures.

3.1. Analogy to the Mars 2020 and ExoMars Landing Sites

The Mars 2020 and ExoMars rovers both carry near-infrared reflectance spectrometers that operate or will operate on the surface of Mars. In terrestrial laboratories, samples to be analyzed by VNIR spectrometers are usually ground into fine powders to homogenize the sample and increase the signal values. This step will not be achieved on the surface of Mars by the two rovers, where natural, unprocessed surfaces will be observed—or roughly crushed rocks in the case of ExoMars' MicrOmega imaging spectrometer (Bibring et al., 2017). Our database is focused on compact rock spectra, providing a physical state analogy between terrestrial and Martian samples to be analyzed.

The Perseverance rover of the Mars 2020 mission has landed on Mars in 2021 and will investigate for the upcoming years Jezero crater and the Nili Planum region, which from orbit exhibit very diverse mineralogical assemblages (Ehlmann et al., 2008, 2009; Goudge et al., 2015; Mustard et al., 2007; Scheller & Ehlmann, 2020; Tarnas et al., 2019). Various samples from the ROMA database exhibit similarities with Jezero crater and Nili Planum, either spectrally or based on the rock type inferred to be present on the sites. In particular, the olivine-bearing bedrock which widely outcrops in the region (Hoefen et al., 2003; Mandon et al., 2020) shows evidence of alteration into Mg-carbonate and serpentine (Ehlmann et al., 2008, 2009). The ROMA spectra of olivine, magnesite, and serpentine mixtures would allow the investigation of the first-order relative proportion of these minerals in the field of view. The various dark and crater-retaining units possibly interpreted as volcanic in Jezero crater and Nili Planum might be analogous to some volcanic rocks of the database. In particular, of interest for the comparison with the Jezero floor unit, multiple samples from our database exhibit the strong absorption bands typical of pyroxene-bearing rocks (mostly Martian meteorites), which have been detected from orbit over this unit (Goudge et al., 2015; Horgan et al., 2020). Most of the other unaltered igneous rocks included in ROMA show less prominent spectral absorptions, and could be relevant for a comparison with the other potential volcanic units of the region from which no spectral features could be clearly identified from orbit (Mustard et al., 2007; Quantin-Nataf et al., 2018).

The ExoMars landing site Oxia Planum is a hundred of kilometers-wide plateau, where the main geological units identified from orbit are a stratified and fractured basement enriched in Fe/Mg-clay minerals (vermiculite or iron-saponite being the best spectral match), some deltaic deposits with a signature of opaline silica, as well as a spectrally muted dark resistant unit whose origin has been interpreted as potentially volcanic (Carter et al., 2016; Quantin-Nataf et al., 2021). In particular, Mandon, Parkes Bowen, et al. (2021) showed that the clay-bearing unit exhibits a spectral signature consistent with a mixture of olivine in addition to the clay minerals. The mixtures of vermiculite and olivine from the ROMA database provide an analogy with these clay-bearing deposits at Oxia Planum, which are the main targets of the mission and are the most common types of exposures at the site (Quantin-Nataf et al., 2021). The various mixing ratios included in the database would provide a framework for the estimation of the olivine versus clay mineral proportions. In addition, pedogenesis was proposed by Carter et al. (2016) as one of the main mechanisms of basement alteration to explain the widespread occurrence of clay minerals at Oxia Planum. Comparisons with the "SL," "R," and "S" paleosol sample sets would help to

investigate this hypothesis on the ground. Finally, the spectral comparison between the wide range of igneous rocks from the ROMA database and the dark resistant unit of potential volcanic origin might help constrain its mineralogical composition.

3.2. Phase Detectability and Band Depth/Mineralogical Proportion Relationship

The spectra of natural rocks included in ROMA can be used to study the complex effects of mineralogical mixtures and surface state and their implications on the interpretation of planetary surfaces reflectance spectra. In particular, the following effects are observed:

1. in the igneous rock data set, a considerable amount of rocks are estimated as relatively fresh: XRD analysis might reveal the presence of minor secondary minerals, but these rocks do not exhibit a visible/evident physical or chemical alteration and rather display an undisturbed texture with the prevalence of igneous minerals. However, these rocks often exhibit reflectance spectra dominated by the spectral features of alteration minerals (e.g., UCB18), similarly to highly altered samples. This has been noted in previous studies on synthetic mixtures (e.g., Thollot, 2013), but is a major issue for the interpretation of the nature, origin, and history of planetary surfaces, as a weakly altered igneous rock might have similar spectral features as a highly altered rock or a sediment mostly composed of non-igneous minerals. Therefore, the ROMA library could be used to further investigate whether the origin of rocks of similar composition might be discriminated based on specific spectral features. To this aim, the spectra of intact rocks are indeed needed, as any texture that might be indicative of the rock nature (e.g., the presence of a cement for a sedimentary rock) and that could potentially have a signature in the spectral signal would be lost during crushing
2. amongst the mafic rocks which do not exhibit the absorption bands related to secondary minerals, only the samples with pyroxene or olivine phenocrysts have spectra showing the corresponding absorption bands (i.e., when pyroxene and olivine are present as small crystals, they are not readily detected). This effect is expected: in a slab rock, particles are, as opposed to powders, welded together and optical coupling is likely to dominate (Hapke, 1993). In this regime, particles are close within a wavelength of each other, which reduces reflections. This usually yields flat and low reflectance spectra for intact rocks compared to their powder equivalent (e.g., Carli et al., 2015). However, with increasing grain size, the absorption of minerals increases, which leads to a higher probability of observing absorption bands related to specific minerals in the rock spectra

These observations emphasize the nonlinear behavior of the absorption band depth with respect to the mineralogical proportion in the rock and the grain size. These effects should be carefully considered when interpreting the reflectance spectra of rocks and soils on planetary surfaces.

Of interest for the sites explored by the Perseverance and Rosalind Franklin rovers, the synthetic mixtures spectra in ROMA provide an insight into the detectability of the various phases observed on the landing sites as well as the evolution of their associated absorption bands depth with respect to mineralogical proportion (Figures 3f, 3g and 3h). As the phases present on the landing sites might not share the exact same composition and grain size distribution, likely contain other phases not detected from orbit, and might not be measured with the same illumination and observation geometries, great caution should be applied when discussing the following results, and the values discussed in this section should be considered as first-order estimations. These results could also be transposed to orbital spectral data, but we encourage the reader to keep in mind that complex effects of spectral mixing, scaling between in situ and orbital measurements, and surface properties (e.g., granulometry, crystallinity) occur, and that analogy between these two types of data sets might be limited (e.g., Dehouck et al., 2020; Pan et al., 2021; Rampe et al., 2018; Salvatore et al., 2020).

1. The spectral results on the olivine/carbonate mixtures show that the coarse-grained olivine present in Jezero crater and Nili Fossae is potentially detectable with reflectance spectrometry (i.e., when a distinct absorption at ∼1 μm is observed) when present in the measurement spot at more than ∼20–40 wt.% relative to carbonate. This value increases with the addition of serpentine: in the triphasic olivine/magnesite/serpentine mixtures, ∼60 wt.% olivine (with equal magnesite/serpentine proportions) in the mixture is required for the 1 μm olivine absorption band to be observed. Mixed with olivine, carbonate, and serpentine have diagnostic absorptions (at ∼2.3 and 2.5 μm for the carbonate and ∼1.4, 1.9, 2.1, 2.3, and 2.5 μm for the serpentine) easily detectable by the spectrometer, the detectability threshold being comprised between ∼1 wt.% and 5 wt.%. In the Nili Fossae region, serpentine is detected over rare outcrops, while carbonate spectral features are commonly observed

(Ehlmann et al., 2009). Our results show that the absorption bands related to serpentine are observed at very low serpentine proportion, implying that carbonate is probably the dominant alteration phase in weight proportion in the region

2. At Oxia Planum, the dominant spectral signal is that of a Fe/Mg-rich clay mineral, while mixtures with olivine are locally observed (Mandon et al., 2021c). If mixed with olivine, the proportion of clay mineral in the outcrops where no olivine is detected should be, by comparison with our measurements, greater than ∼40 wt.% relatively to the olivine proportion, so that the 1 μm absorption band of olivine is masked. Likewise, outcrops where olivine is detected should contain at least ∼60 wt.% olivine for ∼40 wt.% clay mineral, relatively. At lower olivine proportion, the presence of olivine might be inferred by an increase of the spectral continuum reflectance levels, primarily in the 2.2–2.6-μm range where vermiculite is less reflective
3. Finally, our results on kaolinite and Al-rich smectite mixtures show that, for the two landing sites where the spectral 2.2 μm doublet of kaolinite has been observed, kaolinite must be predominant compared to the Al-rich smectite phase, as this doublet is here only observed from 60 wt.% kaolinite

4. Curation and Evolution of the Database

The dedicated website of ROMA is hosted by the Mars System of Information (MarsSI) facility, which is part of the web portal PSUP (Planetary SUrface Portal). MarsSI has been certified as a national observation service by the French Institut National des Sciences de l'Univers (INSU), and is curated by a permanent data engineer at the Observatoire des Sciences de l'Univers de Lyon (OSUL). This will ensure a long-term community access to the ROMA database, which will be permanently accessed at https://roma.univ-lyon1.fr. In the long term, a global and homogenized database will be needed to simplify the search for reference spectra in planetary science. To this aim, the data in ROMA will be integrated in a wider library, the Solid Spectroscopy Hosting Architecture of Databases and Expertise (SSHADE; Mandon, Beck, Quantin-Nataf, Dehouck, Thollot, et al., 2021; Schmitt et al., 2014), which gathers a larger panel of spectroscopic measurements (from gamma to radio wavelength) on various types of materials (ice, minerals, organics, etc.).

In this contribution, we described the current state of this database, which will likely be improved in the future by the authors or from other contributions with additional measurement types (e.g., elemental data) and with new samples relevant for the exploration of Mars, as new rock analogs are available for curation and as our knowledge of the landing sites of the rovers evolves. In particular, the measurements on the following natural rock samples would be a great future addition to the database: marine, lacustrine, and fluvial sediments (possibly present in the landing regions of the Mars 2020 and ExoMars rover missions; Horgan et al., 2020; Quantin-Nataf et al., 2021), olivine-rich pyroclastic deposits (possible analogs to the olivine-bearing rocks investigated by the Perseverance rover; Kremer et al., 2019; Mandon et al., 2020), low-leaching, Fe/Mg-bearing paleosols (possibly present at Oxia Planum; Carter et al., 2016; Mandon, Parkes Bowen, et al., 2021; Quantin-Nataf et al., 2021).

5. Conclusion

The ROMA database, which includes jointed analyses of the reflectance in the VNIR range of rocks and their estimated mineralogical composition, is made publicly available for the community at https://roma.univ-lyon1.fr. The main specificity of this database is to include spectral measurements of unprocessed rock samples (in addition to particulate rock samples), which are more realistic analogs and often have different spectral features than the fine powders usually analyzed in reflectance spectroscopy. The reflectance spectra and band parameters of these rock samples will be valuable data to be compared with the measurements performed by VNIR spectrometers on planetary surfaces, and especially the SuperCam and MicrOmega reflectance spectrometers onboard the Perseverance and Rosalind Franklin Martian rovers.

Data Availability Statement

The data included in ROMA can be freely accessed at https://roma.univ-lyon1.fr (MarsSI/PSUP facility) and are also being incorporated to the SSHADE database (doi:10.26302/SSHADE/ROMA).

Acknowledgments
The authors thank E. Robert, B. Reynard, J.-A. Barrat, F. Moynier, and the Observatoire de Lyon for providing a significant number of samples of this database, as well as R. Vera for dispensing some discussion on XRD analysis and interpretation. S. Potin is greatly acknowledged for the efforts made in building the reflectance instrumental setup. The authors also thank B. Schmitt for integrating ROMA into the SSHADE spectral database. L. Mandon and C. Quantin-Nataf have been supported by the Agence Nationale de la Recherche (ANR, ANR-18-ERC1-0005). P. Beck has been supported by the H2020 European Research Council (ERC, SOLARYS ERC-CoG2017_771691).

References

Beck, P., Barrat, J. A., Gillet, P., Wadhwa, M., Franchi, I. A., Greenwood, R. C., et al. (2006). Petrography and geochemistry of the chassignite Northwest Africa 2737 (NWA 2737). *Geochimica et Cosmochimica Acta*, *70*(8), 2127–2139. https://doi.org/10.1016/j.gca.2006.01.016

Bibring, J.-P., Hamm, V., Pilorget, C., Vago, J. L., & the MicrOmega Team. (2017). The MicrOmega investigation onboard ExoMars. *Astrobiology*, *17*(6–7), 621–626. https://doi.org/10.1089/ast.2016.1642

Bishop, J. L., Perry, K. A., Dyar, M. D., Bristow, T. F., Blake, D. F., Brown, A. J., & Peel, S. E. (2013). Coordinated spectral and XRD analyses of magnesite-nontronite-forsterite mixtures and implications for carbonates on Mars. *Journal of Geophysical Research: Planets*, *118*, 635–650. https://doi.org/10.1002/jgre.20066

Carli, C., Serventi, G., & Sgavetti, M. (2015). VNIR spectral characteristics of terrestrial igneous effusive rocks: Mineralogical composition and the influence of texture. *Geological Society, London, Special Publications*, *401*(1), 139–158. https://doi.org/10.1144/SP401.19

Carli, C., & Sgavetti, M. (2011). Spectral characteristics of rocks: Effects of composition and texture and implications for the interpretation of planet surface compositions. *Icarus*, *211*(2), 1034–1048. https://doi.org/10.1016/j.icarus.2010.11.008

Carter, J., Quantin-Nataf, C., Thollot, P., Loizeau, D., Ody, A., & Lozach, L. (2016). Oxia Planum: A clay-laden landing site proposed for the ExoMars rover mission: Aqueous mineralogy and alteration scenarios. In *47th Lunar and Planetary Science Conference* (pp. 2064). Retrieved from http://adsabs.harvard.edu/abs/2016LPI....47.2064C

Chipera, S. J., & Bish, D. L. (2001). Baseline studies of the clay minerals society source clays: Powder X-ray diffraction analyses. *Clays and Clay Minerals*, *49*(5), 398–409. https://doi.org/10.1346/CCMN.2001.0490507

Clark, R. N., & Roush, T. L. (1984). Reflectance spectroscopy: Quantitative analysis techniques for remote sensing applications. *Journal of Geophysical Research*, *89*(B7), 6329–6340. https://doi.org/10.1029/JB089iB07p06329

Cloutis, E., Craig, M., Kaletzke, L., McCormack, K., & Stewart, L. (2006). HOSERLab: A new planetary Spectrophotometer facility. In *37th Annual Lunar and Planetary Science Conference* (pp. 2121). Retrieved from https://ui.adsabs.harvard.edu/abs/2006LPI.37.2121C

Crown, D. A., & Pieters, C. M. (1987). Spectral properties of plagioclase and pyroxene mixtures and the interpretation of lunar soil spectra. *Icarus*, *72*(3), 492–506. https://doi.org/10.1016/0019-1035(87)90047-9

Dehouck, E., Cousin, A., Mangold, N., Frydenvang, J., Gasnault, O., David, G., et al. (2020). Is the clay-bearing unit distinct in Gale crater? Geochemical alteration revealed by MSL and ChemCam at Glen Torridon, Mars. In *51st Lunar and Planetary Science Conference* (Abstract #2770).

De Sanctis, M. C., Altieri, F., Ammannito, E., Biondi, D., De Angelis, S., Meini, M., et al. (2017). Ma_miss on ExoMars: Mineralogical characterization of the Martian subsurface. *Astrobiology*, *17*(6–7), 612–620. https://doi.org/10.1089/ast.2016.1541

Dypvik, H., Hellevang, H., Krzesińska, A., Sætre, C., Viennet, J.-C., Bultel, B., et al. (2021). The Planetary Terrestrial Analogues Library (PTAL)—An exclusive lithological selection of possible Martian earth analogues. *Planetary and Space Science*, *208*, 105339. https://doi.org/10.1016/j.pss.2021.105339

Ehlmann, B. L., Mustard, J. F., Murchie, S. L., Poulet, F., Bishop, J. L., Brown, A. J., et al. (2008). Orbital identification of carbonate-bearing rocks on Mars. *Science*, *322*(5909), 1828–1832. https://doi.org/10.1126/science.1164759

Ehlmann, B. L., Mustard, J. F., Swayze, G. A., Clark, R. N., Bishop, J. L., Poulet, F., et al. (2009). Identification of hydrated silicate minerals on Mars using MRO-CRISM: Geologic context near Nili Fossae and implications for aqueous alteration. *Journal of Geophysical Research*, *114*, E00D08. https://doi.org/10.1029/2009JE003339

Fouchet, T., Reess, J.-M., Montmessin, F., Hassen-Khodja, R., Nguyen-Tuong, N., Humeau, O., et al. (2021). The SuperCam infrared spectrometer for the Perseverance rover of the Mars2020 mission. *Icarus*, *373*, 114773. https://doi.org/10.1016/j.icarus.2021.114773

Goudge, T. A., Mustard, J. F., Head, J. W., Fassett, C. I., & Wiseman, S. M. (2015). Assessing the mineralogy of the watershed and fan deposits of the Jezero crater paleolake system, Mars. *Journal of Geophysical Research: Planets*, *120*, 775–808. https://doi.org/10.1002/2014JE004782

Guennelon, R. (1962). Les argiles du bassin de Mormoiron (Vaucluse) et les phenomenes pedologiques anciens. *Annales Agronomiques*, *13*, 363–372.

Hapke, B. (1993). *Theory of reflectance and emittance spectroscopy*. https://doi.org/10.1017/CBO9780511524998

Harloff, J., & Arnold, G. (2001). Near-infrared reflectance spectroscopy of bulk analog materials for planetary crust. *Planetary and Space Science*, *49*(2), 191–211. https://doi.org/10.1016/S0032-0633(00)00132-X

Herd, C. D. K., Walton, E. L., Agee, C. B., Muttik, N., Ziegler, K., Shearer, C. K., et al. (2017). The Northwest Africa 8159 Martian meteorite: Expanding the Martian sample suite to the early Amazonian. *Geochimica et Cosmochimica Acta*, *218*, 1–26. https://doi.org/10.1016/j.gca.2017.08.037

Hoefen, T. M., Clark, R. N., Bandfield, J. L., Smith, M. D., Pearl, J. C., & Christensen, P. R. (2003). Discovery of olivine in the Nili Fossae region of Mars. *Science*, *302*(5645), 627–630. https://doi.org/10.1126/science.108964

Horgan, B. H. N., Anderson, R. B., Dromart, G., Amador, E. S., & Rice, M. S. (2020). The mineral diversity of Jezero crater: Evidence for possible lacustrine carbonates on Mars. *Icarus*, *339*, 113526.

Horgan, B. H. N., Cloutis, E. A., Mann, P., & Bell, J. F. (2014). Near-infrared spectra of ferrous mineral mixtures and methods for their identification in planetary surface spectra. *Icarus*, *234*, 132–154. https://doi.org/10.1016/j.icarus.2014.02.031

Hubbard, C. R., & Snyder, R. L. (1988). RIR—Measurement and use in quantitative XRD. *Powder Diffraction*, *3*(2), 74–77. https://doi.org/10.1017/S0885715600013257

Kokaly, R. F., Clark, R. N., Swayze, G. A., Livo, K. E., Hoefen, T. M., Pearson, N. C., et al. (2017). *USGS spectral library version 7 (USGS numbered series No. 1035)*. U.S. Geological Survey. Retrieved from http://pubs.er.usgs.gov/publication/ds1035

Korablev, O. I., Dobrolensky, Y., Evdokimova, N., Fedorova, A. A., Kuzmin, R. O., Mantsevich, S. N., et al. (2017). Infrared spectrometer for ExoMars: A mast-mounted instrument for the rover. *Astrobiology*, *17*(6–7), 542–564. https://doi.org/10.1089/ast.2016.1543

Kremer, C. H., Mustard, J. F., & Bramble, M. S. (2019). A widespread olivine-rich ash deposit on Mars. *Geology*, *47*(7), 677–681. https://doi.org/10.1130/G45563.1

Lantz, C., Poulet, F., Loizeau, D., Riu, L., Pilorget, C., Carter, J., et al. (2020). Planetary terrestrial analogues library project: 1. Characterization of samples by near-infrared point spectrometer. *Planetary and Space Science*, *189*, 104989. https://doi.org/10.1016/j.pss.2020.104989

Mandon, L. (2020). *Préparation des futures missions in situ martiennes via la télédétection et l'expérimentation en spectroscopie de réflectance* (These de doctorat, Lyon). Retrieved from https://www.theses.fr/2020LYSE1261

Mandon, L., Beck, P., Quantin-Nataf, C., Dehouck, E., Pommerol, A., Yoldi, Z., et al. (2021). Martian meteorites reflectance and implications for rover missions. *Icarus*, *366*, 114517. https://doi.org/10.1016/j.icarus.2021.114517

Mandon, L., Beck, P., Quantin-Nataf, C., Dehouck, E., Thollot, P., Loizeau, D., & Volat, M. (2021). *SSHADE/ROMA: ROck reflectance for MArtian in situ exploration database*. SSHADE (OSUG Data Center). Retrieved from https://www.sshade.eu/doi/10.26302/SSHADE/ROMA

Mandon, L., Parkes Bowen, A., Quantin-Nataf, C., Bridges, J. C., Carter, J., Pan, L., et al. (2021). Morphological and spectral diversity of the clay-bearing unit at the ExoMars landing site Oxia Planum. *Astrobiology*, *21*(4). 464–480. https://doi.org/10.1089/ast.2020.2292

Mandon, L., Quantin-Nataf, C., Thollot, P., Mangold, N., Lozac'h, L., Dromart, G., et al. (2020). Refining the age, emplacement and alteration scenarios of the olivine-rich unit in the Nili Fossae region, Mars. *Icarus*, *336*, 113436. https://doi.org/10.1016/j.icarus.2019.113436

Maurice, S., Wiens, R. C., Bernardi, P., Caïs, P., Robinson, S., Nelson, T., et al. (2021). The SuperCam instrument suite on the Mars 2020 rover: Science objectives and mast-unit description. *Space Science Reviews*, *217*(3), 47. https://doi.org/10.1007/s11214-021-00807-w

McKeown, N., Bishop, J. L., Cuadros, J., Hillier, S., Amador, E., Makarewicz, H. D., et al. (2011). Interpretation of reflectance spectra of clay mineral-silica mixtures: Implications for Martian clay mineralogy at Mawrth Vallis. *Clays and Clay Minerals*, *59*(4), 400–415. https://doi.org/10.1346/CCMN.2011.0590404

McSween, H. Y., Taylor, G. J., & Wyatt, M. B. (2009). Elemental composition of the Martian crust. *Science*, *324*(5928), 736–739. https://doi.org/10.1126/science.1165871

Moll, W. F. (2001). Baseline studies of the clay minerals society source clays: Geological origin. *Clays and Clay Minerals*, *49*(5), 374–380. Retrieved from https://pubs.geoscienceworld.org/ccm/article-abstract/49/5/374/48157/BASELINE-STUDIES-OF-THE-CLAY-MINERALS-SOCIETY

Mustard, J. F., Poulet, F., Head, J. W., Mangold, N., Bibring, J.-P., Pelkey, S. M., et al. (2007). Mineralogy of the Nili Fossae region with OMEGA/Mars express data: 1. Ancient impact melt in the Isidis basin and implications for the transition from the Noachian to Hesperian. *Journal of Geophysical Research*, *112*, E08S03. https://doi.org/10.1029/2006JE002834

Pan, L., Quantin-Nataf, C., Mandon, L., Martinot, M., & Beck, P. (2021). Spectral endmember variability on hyperspectral datasets of a Martian meteorite—Implications for planetary surfaces. *Icarus*, *370*, 114656. https://doi.org/10.1016/j.icarus.2021.114656

Pieters, C. M., & Hiroi, T. (2004). RELAB (reflectance experiment laboratory): A NASA multiuser spectroscopy facility. In *35th Lunar and Planetary Science Conference* (pp. 1720). Retrieved from https://ui.adsabs.harvard.edu/abs/2004LPI....35.1720P

Pompilio, L., Sgavetti, M., & Pedrazzi, G. (2007). Visible and near-infrared reflectance spectroscopy of pyroxene-bearing rocks: New constraints for understanding planetary surface compositions. *Journal of Geophysical Research*, *112*, E01004. https://doi.org/10.1029/2006JE002737

Potin, S., Brissaud, O., Beck, P., Schmitt, B., Magnard, Y., Correia, J.-J., et al. (2018). SHADOWS a spectro-gonio radiometer for bidirectional reflectance studies of dark meteorites and terrestrial analogs: Design, calibrations, and performances on challenging surfaces. *Applied Optics*, *57*(28), 8279–8296. https://doi.org/10.1364/AO.57.008279

Poulet, F., Mangold, N., Platevoet, B., Bardintzeff, J.-M., Sautter, V., Mustard, J., et al. (2009). Quantitative compositional analysis of Martian mafic regions using the MEx/OMEGA reflectance data: 2. Petrological implications. *Icarus*, *201*(1), 84. https://doi.org/10.1016/j.icarus.2008.12.042

Quantin-Nataf, C., Carter, J., Mandon, L., Thollot, P., Balme, M., Volat, M., et al. (2021). Oxia Planum: The landing site for the ExoMars "Rosalind Franklin" rover mission: Geological context and prelanding interpretation. *Astrobiology*, *21*(3), 345–366. https://doi.org/10.1089/ast.2019.2191

Quantin-Nataf, C., Dromart, G., & Mandon, L. (2018). Noachian to Amazonian volcanic activity in NE Syrtis region. In *49th Lunar and Planetary Science Conference* (Abstract #2591). Retrieved from http://adsabs.harvard.edu/abs/2018LPI....49.2591Q

Rampe, E. B., Lapotre, M. G. A., Bristow, T. F., Arvidson, R. E., Morris, R. V., Achilles, C. N., et al. (2018). Sand mineralogy within the Bagnold Dunes, Gale Crater, as observed in situ and from orbit. *Geophysical Research Letters*, *45*, 9488–9497. https://doi.org/10.1029/2018GL079073

Salvatore, M. R., Fraeman, A. A., Gasda, P. J., Rampe, E. B., Gabriel, T. S. J., Gasnault, O., et al. (2020). Lessons learned when reconciling orbital and in situ exploration of Vera Rubin ridge, Gale crater, Mars. In *51st Lunar and Planetary Science Conference*. (Abstract #2714). Retrieved from http://adsabs.harvard.edu/abs/2020LPI....51.2714S

Sautter, V., Barrat, J. A., Jambon, A., Lorand, J. P., Gillet, P., Javoy, M., et al. (2002). A new Martian meteorite from Morocco: The nakhlite North West Africa 817. *Earth and Planetary Science Letters*, *195*(3), 223–238. https://doi.org/10.1016/S0012-821X(01)00591-X

Sautter, V., Toplis, M. J., Wiens, R. C., Cousin, A., Fabre, C., Gasnault, O., et al. (2015). In situ evidence for continental crust on early Mars. *Nature Geoscience*, *8*(8), 605–609. https://doi.org/10.1038/ngeo2474

Scheller, E. L., & Ehlmann, B. L. (2020). Composition, stratigraphy, and geological history of the Noachian basement surrounding the Isidis impact basin. *Journal of Geophysical Research: Planets*, *125*, e2019JE006190. https://doi.org/10.1029/2019JE006190

Schmitt, B., Albert, D., Bollard, P., Bonal, L., Gorbacheva, M., Beck, P., & Quirico, E. (2014). The SSHADE project: An European database infrastructure in solid spectroscopy. In *European planetary science Congress* (Vol. 9, Abstract #581).

Tarnas, J. D., Mustard, J. F., Lin, H., Goudge, T. A., Amador, E. S., Bramble, M. S., et al. (2019). Orbital identification of hydrated silica in Jezero crater, Mars. *Geophysical Research Letters*, *46*, 12771–12782. https://doi.org/10.1029/2019GL085584

Thollot, P. (2013). *Etude de l'altération de la surface de Mars par imagerie hyperspectrale: Minéralogie des régions de Noctis Labyrinthus et Valles Marineris*. (Doctoral dissertation, Nantes). Retrieved from http://www.theses.fr/2013NANT2076

Wiens, R. C., Maurice, S., Robinson, S. H., Nelson, A. E., Cais, P., Bernardi, P., et al. (2021). The SuperCam instrument suite on the NASA Mars 2020 rover: Body unit and combined system tests. *Space Science Reviews*, *217*(1), 4. https://doi.org/10.1007/s11214-020-00777-5